Hindawi
Advances in Civil Engineering
Volume 2021, Article ID 3919281, 11 pages
https://doi.org/10.1155/2021/3919281

Research Article

Evaluation of Seismic Site Amplification Using 1D Site Response Analyses at Ba Dinh Square Area, Vietnam

Ngoc-Long Tran,[1] Muhammad Aaqib,[2] Ba-Phu Nguyen,[3] Duy-Duan Nguyen,[1] Viet-Linh Tran,[1] and Van-Quang Nguyen[1]

[1]*Department of Civil Engineering, Vinh University, Vinh 461010, Vietnam*
[2]*Department of Civil Engineering, National University of Technology, Islamabad, Pakistan*
[3]*Department of Civil Engineering, Industrial University of Ho Chi Minh City, Ho Chi Minh City 700000, Vietnam*

Correspondence should be addressed to Van-Quang Nguyen; nguyenvanquang240484@gmail.com

Received 15 June 2021; Revised 9 August 2021; Accepted 18 August 2021; Published 30 August 2021

Academic Editor: Cemal Ozer Yigit

This study presents a case study on ground response analysis of one of the important cultural heritages in Hanoi, Vietnam. One-dimensional nonlinear and equivalent linear site response analyses which are commonly applied to solve the problem of seismic stress wave propagation are performed at the Ba Dinh square area. A measured in-situ shear wave velocity profile and corresponding geotechnical site investigation and laboratory test data are utilized to develop the site model for site-specific ground response analysis. A suite of earthquake records compatible with Vietnamese Design Code TCVN 9386: 2012 rock design spectrum is used as input ground motions at the bedrock. A few concerns associated with site-specific ground response evaluation are analyzed for both nonlinear and equivalent linear procedures, including shear strains, mobilized shear strength, and peak ground acceleration along with the depth. The results show that the mean maximum shear strains at any soil layer are less than 0.2% in the study area. A deamplification portion within the soil profile is observed at the layer interface with shear wave velocity reversal. The maximum peak ground acceleration (PGA) at the surface is about 0.2 g for equivalent linear analysis and 0.16 g for nonlinear analysis. The ground motions are amplified near the site natural period 0.72 s. The soil factors calculated in this study are 1.95 and 2.07 for nonlinear and equivalent linear analyses, respectively. These values are much different from the current value of 1.15 for site class C in TCVN 9386: 2012. A comparison of calculated response spectra and amplification factors with the local standard code of practice revealed significant discrepancies. It is demonstrated that the TCVN 9386: 2012 soil design spectrum is unable to capture the calculated site amplification in the study area.

1. Introduction

Seismic hazard assessment is needed for seismically active regions and plays a significant role in the sustainable development of urban infrastructure. Ground response analyses are commonly employed for this purpose [1].

Vietnam is located in the center of Southeast Asia and is strongly affected by relative movements between the Mediterranean and Himalaya belts [2]. Hanoi is the capital of Vietnam and lies on two main faults, which are the Red River fault and the Chay River fault. These faults belong to the Red River Shear Zone that comes from Tibet and runs more than 1000 km to the Gulf of Tonkin (located off the coasts of North Vietnam and South China). The Red River fault is also considered as the border of the Indochina Plate and the South China Plate. Recently, the geodynamic research in the Hanoi basin shows that the Red River fault is reactivated [3–5]. Besides, Hanoi is also affected by nearby active faults such as the Lai Chau-Dien Bien (LC-DB), Ma River, Son La, Lo River, and Chay River faults as shown in Figure 1 [6, 7].

From 114 to 2003, a total of 1645 earthquakes, either by measurement or by studying the historical archives, were recorded in Vietnam with a local magnitude (M_L) of 3 or higher [8]. The typical earthquakes that occurred in the

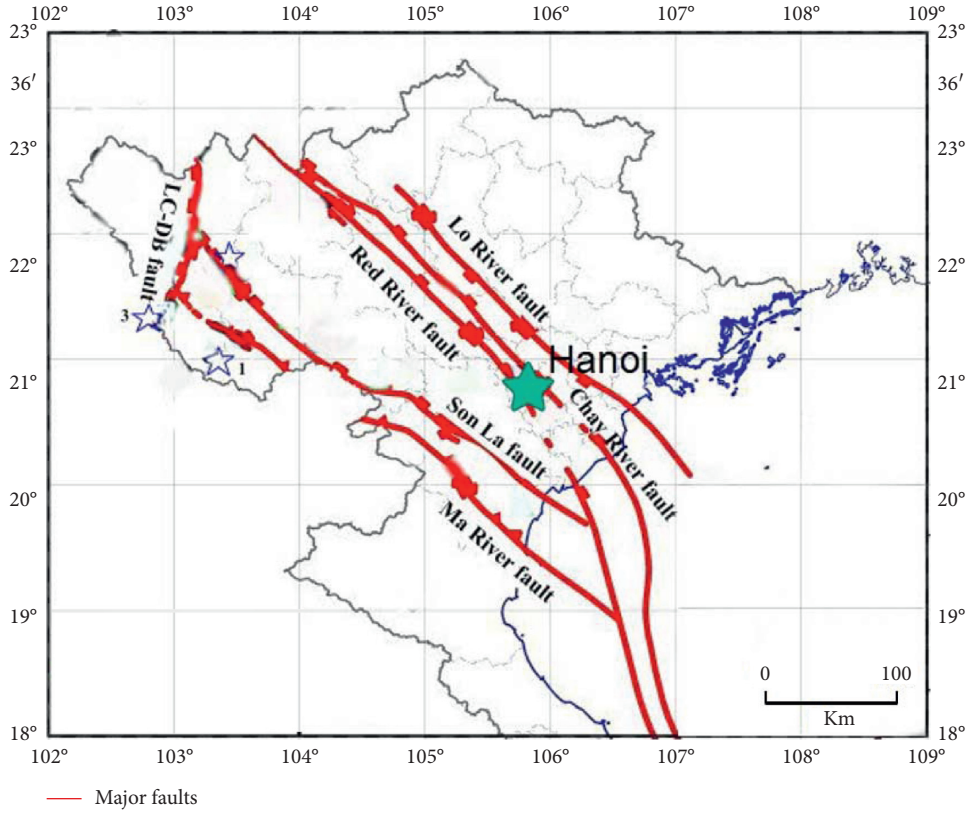

Figure 1: Major faults related to the Hanoi region [6, 7].

northern part of Vietnam nearby the Hanoi are the Dienbien earthquake (1935, $M_L = 6.75$, Ma River fault) and the Tuangiao earthquake (1983, $M_L = 6.75$, Son La fault) [9]. Recently, the earthquake activity was recorded in the adjacent provinces of the capital, Hanoi. These include Dien Bien in 2001, Ha Giang in 2005, Ninh Binh in 2005, and Hoa Binh in 2010 with a M_L of 5.3, 4.7, 3.1, and 4.0, respectively. They caused vibration and damage to buildings in Hanoi. Furthermore, in the past, three earthquakes were recorded at Hanoi in 1276, 1278, and 1285 with $M_L = 5.5$–6.0 [7].

The study of Nhung and Phuong [10] presented that the geology of Hanoi is mainly site classes D, E, F according to EC-8 [11]. The surface is mainly sandy and clay sediments in Holocene or Pleistocene. The bottom of Holocene deposits is at a depth of 10–45 m. The bottom of Pleistocene deposits is at a depth of 45 m (in the north of Hanoi) to 110 m (in the south of Hanoi) [5]. With the seismic and geological conditions, it revealed that a high amplification can occur in Hanoi. A site-specific study is needed to carry out (i.e. seismic hazard analysis), especially at important locations such as the Ba Dinh square area which includes the President's place and One Pillar Pagoda.

One-dimensional (1D) ground response analysis is commonly performed to evaluate the seismic hazard of the site-specific area [12–15]. Shylamoni et al. [12] evaluated ground response at the Kashiwazaki-Kariwa Nuclear Power Plant site (Japan). Mahmood et al. [13] implemented equivalent linear and nonlinear site response analysis of Pashto Cultural Museum Peshawar, Pakistan. Satyam and Towhata [14] assessed the ground response and liquefaction of the Vijayawada city (India). Aaqib et al. [15] Aaqib et al. [16] investigated the strength correction effect of sites in Korea. Recently, several studies have examined seismic hazard assessment of the Hanoi region ground [2, 7, 17, 18]. Alexandr and Chi [2] and Nhung et al. [17] accessed the liquefaction possibility. Wen et al. [18] and Nguyen et al. [7] reported that sites in the Hanoi area may experience a high amplification and site-specific site response analysis was recommended. This is because the Eurocode-8 (EC-8) [11] forms the basis of the current Vietnamese design code, TCVN 9386: 2012 [19]. The soil factors and the design spectrum used from EC-8 may not be suitable for the geological conditions of Vietnam. In addition, a range of ground motion characteristics such as frequency content and the magnitude has not been investigated yet in the previous studies.

This study performs a site-specific analysis and aims to develop a design spectrum for the Ba Dinh square area where the most important historical, cultural, and government buildings in Vietnam are located. A representative soil profile with a comprehensive site and laboratory investigation is utilized. A suite of input ground motions compatible with the site class A design spectrum in TCVN 9386: 2012 are used. The amplification and shear strain characteristics of the area are studied. Discrepancies with the local standard design of practice are also discussed.

2. The Importance of the Ba Dinh Square Area

Located in the heart of Hanoi, the Ba Dinh square is the largest square in the Ba Dinh district, Vietnam, with a dimension of 550 m (length) and 300 m (width). The square is the historical destination where the Ho Chi Minh Mausoleum was built. Ho Chi Minh is considered the founder of the Democratic Republic of Vietnam. This square also locates many important buildings around it, including the President's Palace, the Ministry of Foreign Affairs, the Ministry of Planning and Investment, and the National Assembly Building. Cultural-historical buildings such as One Pillar Pagoda, the Imperial Citadel of Thang Long (UNESCO World Heritage Site), and the Ho Chi Minh Museum are set nearby. The location of the Ba Dinh square area is shown in Figure 2. It should be added that One Pillar Pagoda is a historic Buddhist temple in Hanoi. It is regarded, alongside the Perfume Temple, as one of Vietnam's two most iconic temples. Thang Long Citadel is a complex of historic imperial buildings and was made a UNESCO World Heritage Site in 2010. It is also known as Hanoi Citadel.

The ground in the Ba Dinh district is mainly site class E according to EC-8 [10]. The Ba Dinh district soil strata typically include four layers [20]. The first layer is river, lake or marsh sediment. The thickness of this layer can be reached to 10 m near the river or lake and 0–0.5 m at other locations. It is followed by white stiff clay, clay mixed with pebbles, and gritstone or sandstone. The thickness of these layers is 10–35 m, 10–20 m, and 5–30 m, respectively. Furthermore, this square is very close to the Red River fault and is only 2.3 km away. The Red River has been shown to have the potential to cause earthquakes with $M_L = 7\text{-}8$ [21]. Therefore, it is important to clarify the significance of ground responses in this area.

3. Soil Profile

A site investigation was performed to characterize the soil profile. The location of the borehole is shown in Figure 2(b). Boring logs show that the depth to the bedrock is approximately 35 m. The site consists of fill, sandy clay, clayey sand, and sand. Shear wave velocity profile and soil properties are presented in Figure 3 and Table 1, respectively. The site natural period (T_s) is 0.72 s; the time-averaged shear wave velocity to 30 m depth (V_{S30}) is 181 m/s and considered as site class C according to EC-8 and TCVN 9386: 2012. It should be noted that the site class of the Ba Dinh square is different than the typical site class in Ba Dinh district. The groundwater level has a significant effect on the ground response, and hence it is taken into account in this study. The water table is located at a depth of 9 m below the ground surface.

4. Input Ground Motions

Owing to a lack of recorded motions in the Ba Dinh square area, a total of 15 input motions from 12 earthquake events used in the study of Nguyen et al. [7] are adopted in this study. Notably, two acceleration-time history components (i.e. North-South and East-West) of earthquake events 5th, 8th, and 10th were used. The NGA-west2 database (http://ngawest2.berkeley.edu/) was utilized to select the ground motions. The target characteristics of the selected motions are compatible with those of the Hanoi city such as moment magnitude (M_w) of 5.5–7.0, rupture distance (R_{rup}) from 0.90 to 85 km, and V_{S30} of 760–1500 m/s. The selected input ground motions were scaled to 0.0976 g which is the representative shaking intensity level for an earthquake return period of 475 years for the Ba Dinh district [19]. The ground motions were selected such that the mean response spectrum matches the target spectrum of site class A in TCVN 9386: 2012 [19], as shown in Figure 4. Table 2 presents in detail the characteristics of the selected earthquake events.

5. One-Dimensional Ground Response Analysis

The pattern of damage in urban areas during an earthquake depends on the characteristics of the event and interaction between site response and the vulnerability of the built structure. Most of the urban settlements have occurred along river valleys with soft and young soil deposits which were prone to severe damage during the earthquake [14]. The Ba Dinh square area is located nearby the Red River; the site-specific response analysis will help predict the local site effects and approximating the dynamic behavior of soil during seismic loading.

One-dimensional equivalent linear (EQL) and nonlinear (NL) response analysis is performed using DEEPSOIL v7.0 [22] in this study. This program has been widely used in previous studies [7, 16, 23–26]. One-dimensional site response analysis is the process of propagating shear waves numerically from the reference rock through the overlying soil layers to the surface. One-dimensional site response allows vertical propagation of shear waves, and soil deposits are assumed as horizontally homogeneous layers. Conventionally, all the site response procedures require the specification of acceleration-time history, and a suite of input motions is usually applied to develop a statistically stable response. EQL is a method in which stiffness and damping of soil layers are calculated for a given shear strain based on EQL iterative procedure [1]. In the case of NL, the dynamic soil properties are determined by the stress–strain relationship at each time step of the loading. A recently developed Generalized Quadratic/Hyperbolic (GQ/H) constitutive model [27] implemented in DEEPSOIL v7.0 was used in this study. This is a widely used model in site response analysis [15, 24, 25, 28–30] and can capture an initial shear modulus at zero shear strain as well as a limiting shear strength at large shear strains. The pressure-dependent nonlinear dynamic curves proposed by Darendeli [31] is used to generate dynamic properties of soil layers. The required parameters are over the consolidation ratio (OCR) of 1.0, the coefficient of lateral Earth pressure (K_o) of 0.5, the number of the cycle of loading (N) of 10, and the frequency of the loading (f) of 1.0. The plasticity index (PI) of sand and clay were 0 and 15, respectively. These chosen parameters of Darendeli are widely used in site response analysis as reported in Aaqib et al. [16], Hashash et al. [28], Nguyen et al.

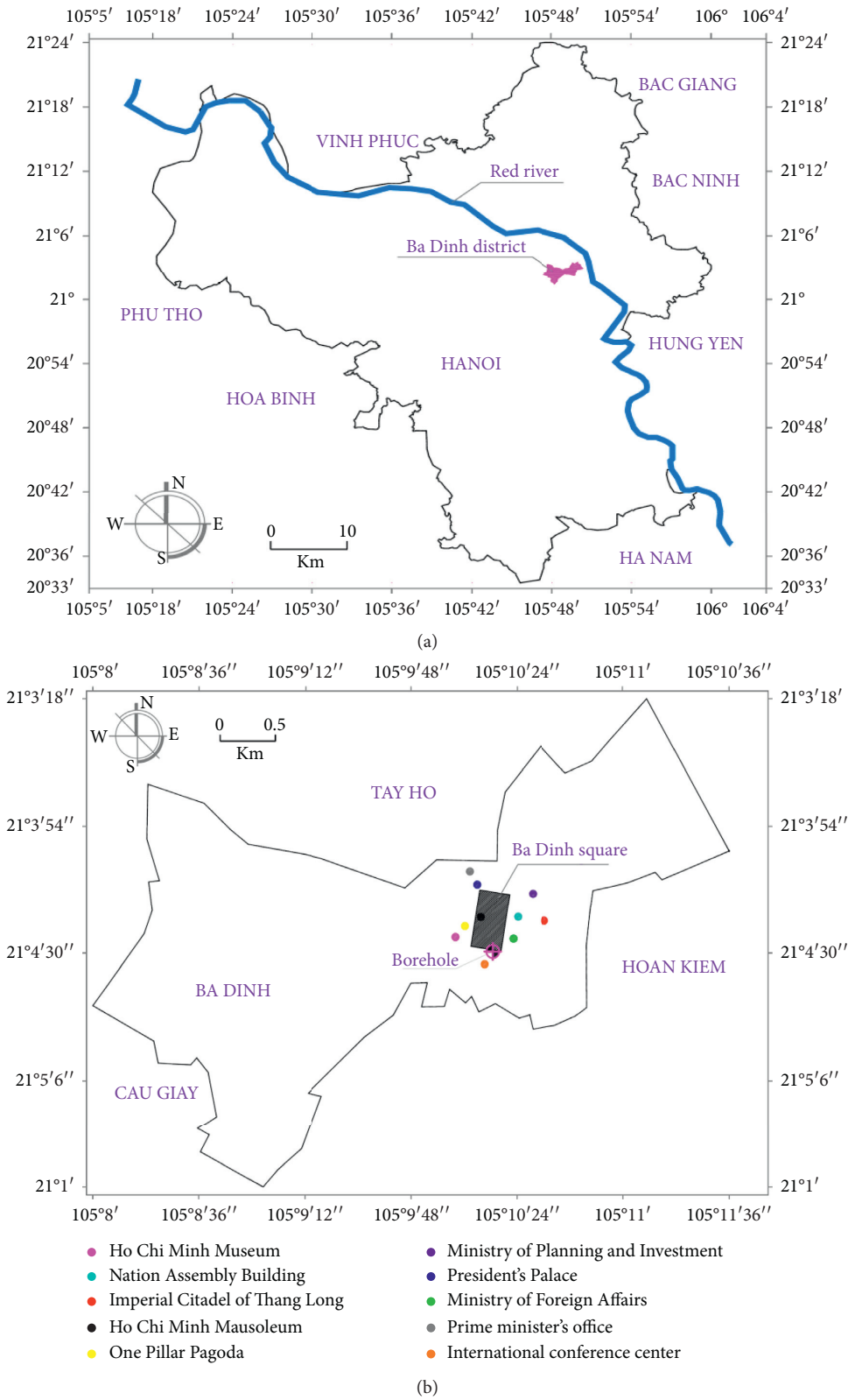

Figure 2: The investigated location: (a) Hanoi city and (b) Ba Dinh district map.

[23], and Nguyen et al. [7]. Figure 5 presents a flowchart of the site response procedure implemented in this study. The flowchart illustrates that a suite of equivalent linear and nonlinear site response analyses are used to determine the site-specific spectral shapes, peak ground acceleration, and maximum shear strain profiles of the Ba Dinh square area.

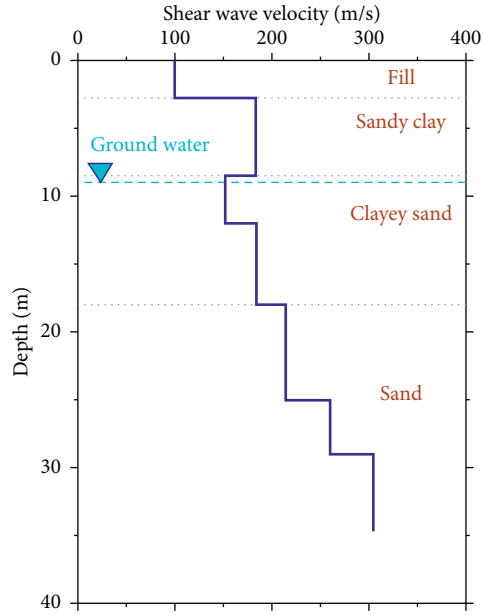

Figure 3: Shear wave velocity profile.

Table 1: Soil properties of the investigated site.

Layer no.	Material type	Thickness (m)	Depth (m)	Density (kg/m^3)	Shear wave velocity (m/s)
1	Fill	2.8	2.8	1650	100
2	Sandy clay	5.7	8.5	1700	184
3	Clayey sand	3.5	12	1800	152
4	Clayey sand	6	18	1800	184
5	Sand	7	25	1900	214
6	Sand	4	29	1900	260
7	Sand	5.5	34.5	1900	304
8	Bedrock	—	—	2250	800

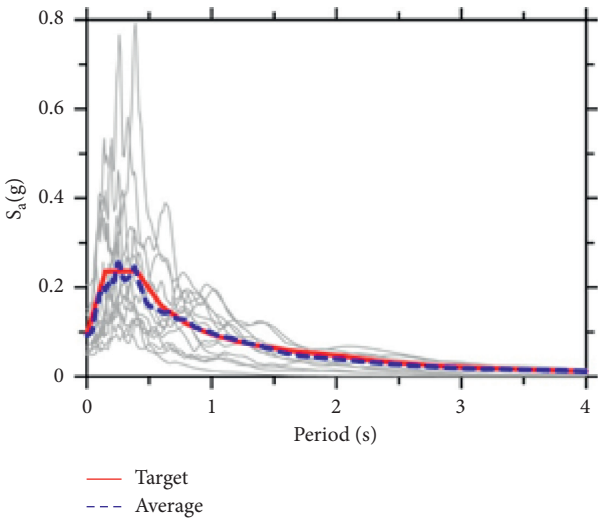

Figure 4: Average input motion and target response spectrum.

Moreover, the amplification factors resulting from this study will provide insights into the discrepancies between the design and site-specific spectra.

6. Results and Discussion

The analysis of induced shear strains is an important factor in any site-specific ground response study. On one hand, in case of the EQL procedure, the initial shear modulus (G_{max}) and damping (D_{min}) of the soil layer are used to calculate the initial shear strain time history. The degraded shear modulus and damping are then calculated using a shear strain of 65%. These soil properties are then subsequently used in the next iterations until the convergence with the target degradation curves is achieved. On the other hand, in the case of the NL procedure, shear stresses are induced at different layers during the propagation of input ground motion from bedrock to the surface, which, in turn, causes shear strains in these soil layers. It is clear that both NL and EQL procedures use distinct ways to calculate the dynamic properties of soil.

Figure 6 presents the variation of shear strains produced by a suite of ground motions with depth for both NL and EQL analyses. Notably, the curves in the gray color in Figures 6 to 8 are the results corresponding to the different ground motions. The solid red line and dashed black line are average results from NL and EQL analyses, respectively. It is demonstrated that the maximum strains calculated by both the procedures differ for a set of ground motions. The NL

Table 2: Selected earthquake ground motions.

No.	Earthquake name	Year	Station	Magnitude (M_w)	Mechanism	R_{rup} (km)	V_{S30} (m/s)	PGA (g)
1	San Fernando	1971	Pasadena-Old Seismo lab	6.61	Reverse	21.5	969.07	0.205
2	Whittier Narrows-01	1987	Pasadena-CIT Kresge lab	5.99	Reverse oblique	18.12	969.07	0.112
3	Loma Prieta	1989	Piedmont Jr high school grounds	6.93	Reverse oblique	73	895.36	0.072
4	Loma Prieta	1989	Point Bonita	6.93	Reverse oblique	83.45	1315.92	0.072
5	Loma Prieta	1989	SF-Pacific heights	6.93	Reverse oblique	75.96	1249.86	0.062
6	Loma Prieta	1989	So. San Francisco_Sierra Pt.	6.93	Reverse oblique	63.15	1020.62	0.054
7	Northridge-01	1994	LA-Wonderland Ave	6.69	Reverse	20.29	1222.52	0.103
8	Northridge-01	1994	Vasquez rocks Park	6.69	Reverse	23.64	996.43	0.151
9	Chi-Chi_ Taiwan-05	1999	TTN042	6.20	Reverse	85.17	845.34	0.060
10	Umbria-03_ Italy	1984	Gubbio	5.60	Normal	15.72	922	0.067
11	Kobe_ Japan	1995	Kobe University	6.90	Strike-slip	0.92	1043	0.312
12	Chi-Chi_ Taiwan-05	1999	HWA002	6.20	Reverse	45.03	789.18	0.029

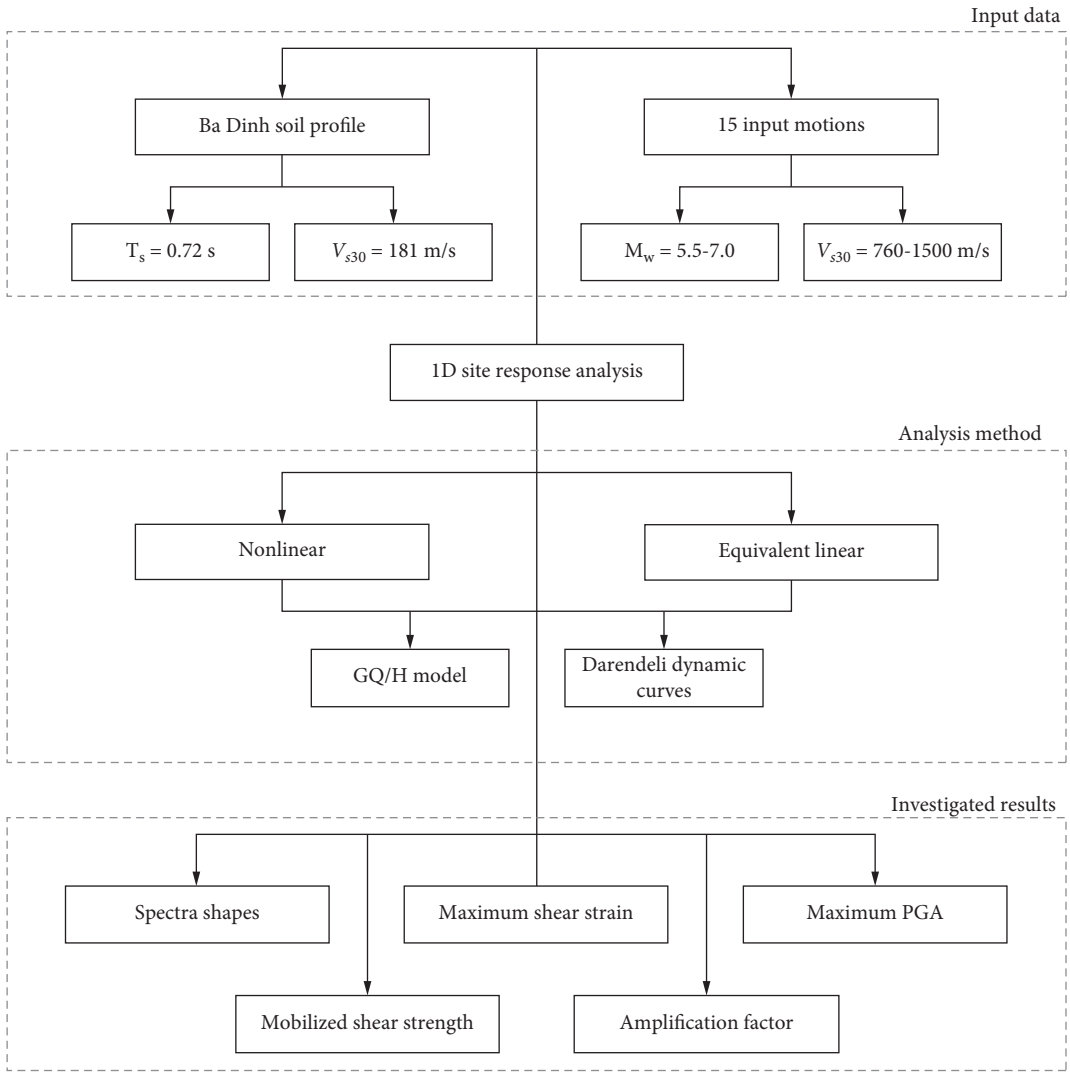

Figure 5: Flow chart of 1D site-specific ground response procedure.

procedure results in maximum strains up to 0.47%, whereas the EQL procedure results in strains up to 0.4%. However, there are insignificant discrepancies in the mean shear strains calculated by both procedures. The average maximum shear strains are encountered at a depth of 11 m in both the procedures and go up to 0.2%. The high strains at

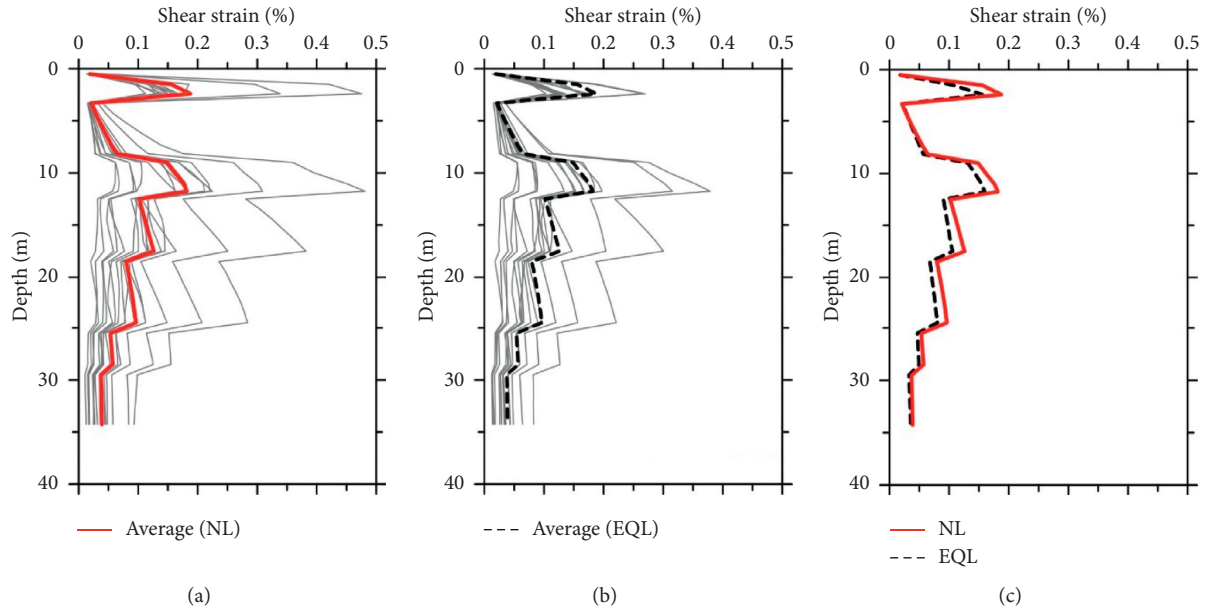

Figure 6: EQL and NL shear strain profile produced by a suite of ground motions.

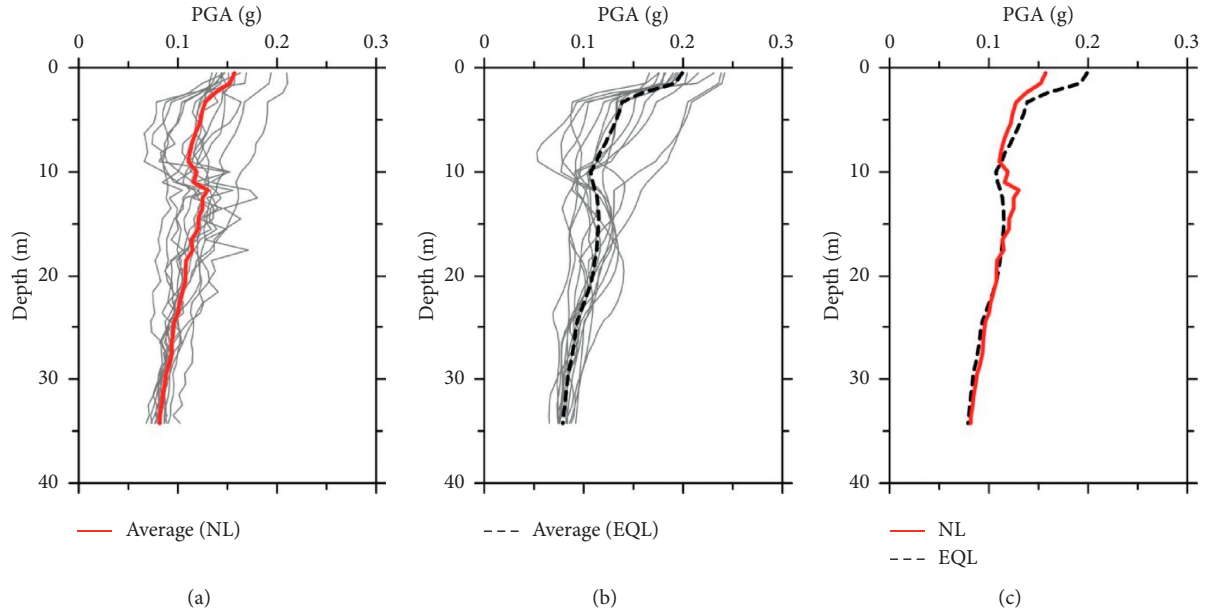

Figure 7: EQL and NL peak ground acceleration profile produced by a suite of ground motions.

11 m are attributed to the presence of shear wave velocity reversal in the soil profile.

Figure 7 presents the variation of peak ground acceleration (PGA) as a function of depth for all the used ground motions and the two procedures. It is demonstrated that PGA increases as the surface is approached, and the peak PGA is observed at the surface by both NL and EQL procedures. The NL procedure calculates surface PGA up to 0.21 g, whereas the EQL results in a peak surface PGA of 0.24 g. The mean surface PGA calculated by the NL procedure is lower than that by the EQL procedure. A deamplification portion is observed at 11 m which is attributed to the presence of shear wave velocity reversal in soil profile at that depth.

Shear strains and shear modulus are also utilized in the calculation of mobilized shear strength. Figure 8 illustrates the mobilized shear strength profiles as a function of depth for all the ground motions. Mobilized shear strength is defined as yield stress developed due to the applied load to resist the deformation of the soil. As a general trend, mobilized shear strength is shown to increase with depth. Some discrepancies are observed where mobilized shear strength

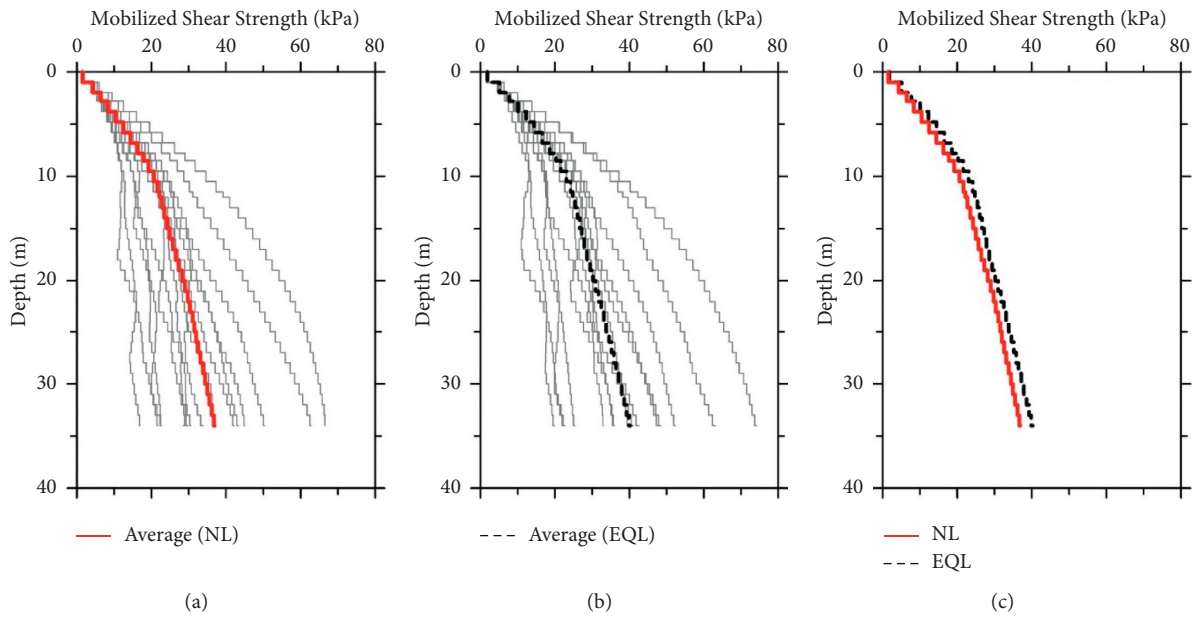

Figure 8: EQL and NL mobilized shear strength profile produced by a suite of ground motions.

reversals are produced by a small set of input motions. In a site-specific study, this behavior is attributed to the use of different shear strains and shear modulus used by each ground motion.

The evaluation of a site for design purposes is most often performed using the acceleration response spectrum. It reflects the frequency content of the ground motion at the surface. Figure 9 depicts the mean surface response spectrum calculated using both the site response procedures. The input response spectrum and the rock code design spectrum (S_A) are also shown. EQL procedure results in a higher response than the NL procedure. A spectral bump is observed at the site natural period of 0.72 s, demonstrating the effect of the site period on amplification.

The amplification factor at a particular spectral period is calculated as the ratio of spectral acceleration at the ground surface and the spectral acceleration at the bedrock. The propagation of seismic waves results in the development of a standing wave at each natural frequency of the soil deposit which causes the amplification at the ground surface. Figure 10 compares the amplification factors calculated from NL and EQL procedures. Peak amplification is observed at the site natural period of 0.9 s in the case of NL analysis, whereas it shifts to 0.72 s in the case of EQL analysis. The soil factor, S, is also calculated and shown in Figure 10. As TCVN 9386: 2012 is based on the Eurocode-8, S is calculated as the average of amplification factors within the interval of 0.05–2.5 s, defined as follows [32]:

$$S = \frac{I_{\text{soil}}}{I_{\text{rock}}}, \tag{1}$$

where I_{soil} and I_{rock} are the spectral acceleration indexes of soil and rock, respectively, defined as follows:

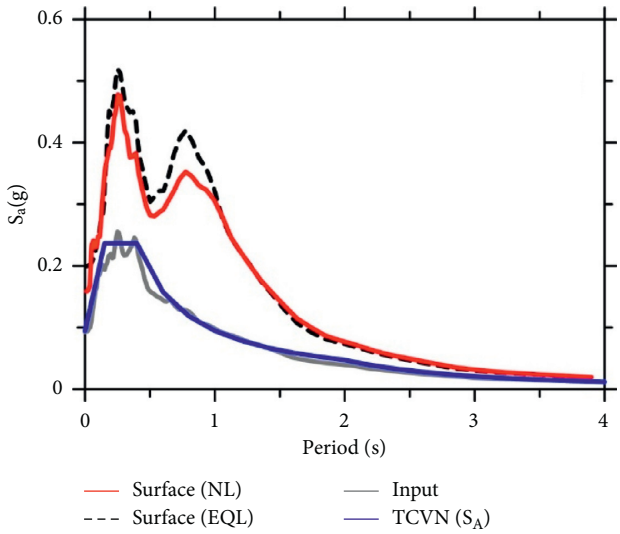

Figure 9: EQL and NL surface response spectra.

$$I_{\text{soil or rock}} = \int_{0.05}^{2.5} S_a(T)\mathrm{d}T, \tag{2}$$

S is calculated as 1.95 by NL and 2.07 by EQL analysis. The calculated soil factor is much higher than that defined in TCVN 9386: 2012 ($S = 1.15$ for ground type C).

Figure 11 compares the calculated mean response spectra and proposed design spectrum with the TCVN 9386: 2012 design spectrum (S_C). The rock design spectrum (S_A) is also shown in this figure. The proposed design spectrum was obtained as a product of the rock design spectrum (S_A) and amplification factor (S). The calculated spectra are higher than the code design spectrum across the whole period

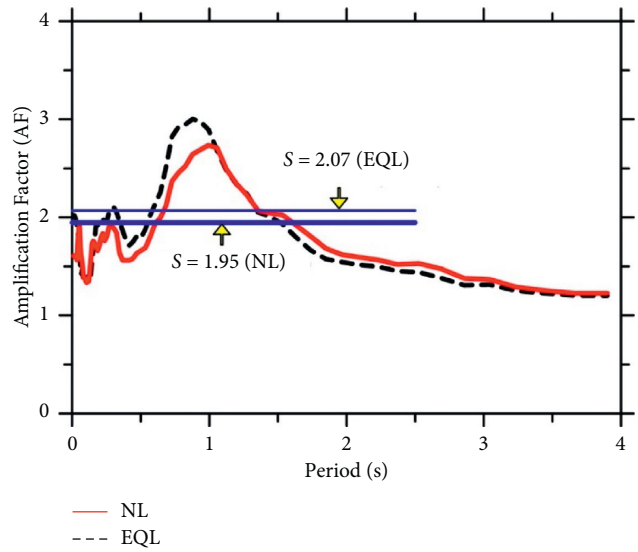

Figure 10: EQL and NL amplification factors.

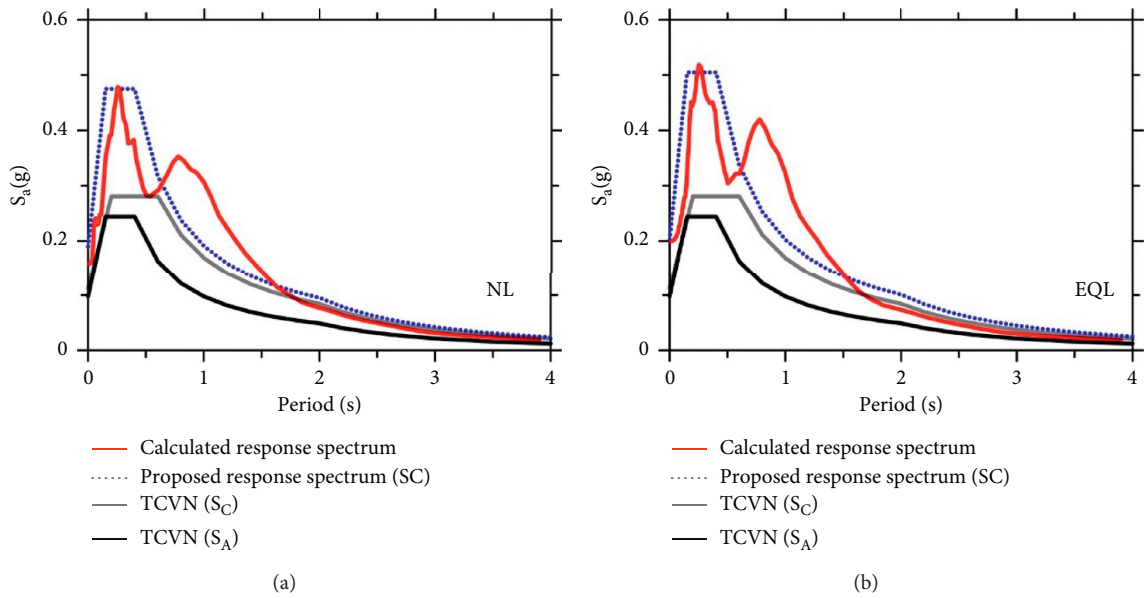

Figure 11: The comparison of the response spectrum of the calculated mean and proposed design with the TCVN 9386: 2012 (S_c): (a) NL, (b) EQL.

range. These questions the applicability of code provisions for Vietnam site conditions, which are primarily based on EC-8. These discrepancies were also reported by Nguyen et al. [7]. The calculated response spectra and proposed design spectrum match favorably except at the spectral periods of 0.65–1.26 s. This is consistent with the results of both NL and EQL approaches. This mismatch is attributed to the use of a single amplification factor for both short-period and long-period range in TCVN 9386: 2012 as well as EC-8. This was also highlighted in the study of Pitilakis et al. [33], where it was recommended that separate amplification factors should be used for short and long periods, as used in NEHRP 2015 provisions [34].

7. Conclusions

This study evaluates ground response at a crucial location in Vietnam which is the Ba Dinh square area. A representative soil profile and 15 compatible earthquake ground motions scaled to the representative design shaking level in the region are used. The one-dimensional nonlinear and equivalent linear site-specific ground response analyses are performed. The results are also compared to the current seismic design code TCVN 9386: 2012. The following conclusions are drawn:

A set of in-situ and laboratory test measurements were utilized. The site under investigation has a V_{S30} of 181 m/s

and is classified as site C according to TCVN 9386: 2012. It is revealed that the site class in the region of study is different from the typical class in the Ba Dinh district (site E).

The NL procedure is usually preferred over the EQL procedure because of its ability to appropriately capture the actual response. Meanwhile, the EQL procedure is cost-effective and easier to apply. However, the EQL procedure was reported to be effective for shear strains <0.4% [35]. In this study, the maximum shear strains calculated by the EQL procedure are less than 0.4%. Therefore, both NL and EQL procedures can be used for the study area. Maximum shear strains in both cases were produced at the interface of the soil layer 2 (sandy clay) and layer 3 (clayey sand) where a shear wave velocity reversal is encountered. The average maximum shear strain reaches up to 2%. Mobilized shear strength is shown to increase as a function of depth.

The PGA profiles were shown to increase as the surface is approached except for the shear wave reversal portion. The average maximum PGA at surface is about 0.2 g and 0.16 g for NL and EQL analyses, respectively. The response spectral comparison indicated that the ground motions are clearly amplified near the site natural period of 0.72 s.

Comparisons of the calculated amplification factor and response spectra with the local design code of practice revealed significant discrepancies across the whole period range. The computed soil factors are 1.95 and 2.07 for NL and EQL analyses, respectively, and they are much higher than that defined in TCVN 9386: 2012 ($S = 1.15$ for ground type C). The calculated response spectra and design spectrum developed using the soil factor calculated in this study also shown discrepancies at the period range 0.65–1.2 s. It is recommended to use different soil factors for both short-period and long-period ranges rather than using a single factor in TCVN 9386: 2012.

Data Availability

The data used to support the findings of this study are available from the corresponding author upon request.

Conflicts of Interest

The authors declare that there are no conflicts of interest regarding the publication of this paper.

References

[1] S. L. Kramer, *Geotechnical Earthquake Engineering*, Prentice-Hall, Upper Saddle River, NJ, USA, 1996.

[2] G. Alexandr and T. N. Chi, "Liquefaction possibility of soil layers during earthquake in Hanoi," *International Journal of GEOMATE*, vol. 13, no. 39, pp. 148–155, 2017.

[3] A. Replumaz, R. Lacassin, P. Tapponnier, and P. Leloup, "Large river offsets and Plio-Quaternary dextral slip rate on the Red river fault (Yunnan, China)," *Journal of Geophysical Research: Solid Earth*, vol. 106, no. B1, pp. 819–836, 2001.

[4] V. Q. Hai, T. Q. Cuong, and N. V. Thuan, "Crustal movement along the Red river fault zone from GNSS data," *Vietnam Journal of Earth Sciences*, vol. 38, no. 1, pp. 14–21, 2016.

[5] G. K. Trung, N. D. Vinh, and D. T. Men, "Soil classification and seismic site response analysis for some areas in Hanoi city," *VNU Journal of Science: Earth and Environmental Sciences*, vol. 34, no. 1, 2018.

[6] L. M. Nguyen, T.-L. Lin, Y. M. Wu et al., "The first peak ground motion attenuation relationships for north of Vietnam," *Journal of Asian Earth Sciences*, vol. 43, no. 1, pp. 241–253, 2012.

[7] V.-Q. Nguyen, M. Aaqib, D.-D. Nguyen, N.-V. Luat, and D. Park, "A site-specific response analysis: a case study in Hanoi, Vietnam," *Applied Sciences*, vol. 10, no. 11, p. 3972, 2020.

[8] T. Ngo, M. Nguyen, and D. Nguyen, "A review of the current Vietnamese earthquake design code," *Electronic Journal of Structural Engineering*, vol. 8, pp. 32–41, 2008.

[9] N. H. Phuong, "Probabilistic assessment of earthquake hazard in Vietnam based on seismotectonic regionalization," *Tectonophysics*, vol. 198, no. 1, pp. 81–93, 1991.

[10] B. T. Nhung and N. H. Phuong, "Local site classification for the urban region of Hanoi city," *Vietnam Journal of Earth Sciences*, vol. 37, no. 4, pp. 363–372, 2015.

[11] Eurocode 8, *Design of Structures for Earthquake Resistance-Part 1: General Rules, Seismic Actions and Rules for Buildings*, Wiley, Hoboken, NJ, USA, 2005.

[12] P. Shylamoni, D. Choudhury, S. Ghosh, A. Ghosh, and P. C. Basu, "Seismic ground response analysis of KK-NPP site in the event of NCO earthquake using DEEPSOIL," in *Proceedings of the Geo-Congress 2014: Geo-Characterization and Modeling for Sustainability*, pp. 840–849, ASCE, Atlanta, GA, USA, February 2014.

[13] K. Mahmood, S. A. Khan, Q. Iqbal, F. Karim, and S. Iqbal, "Equivalent linear and nonlinear site-specific ground response analysis of Pashto cultural museum Peshawar, Pakistan," *Iranian Journal of Science and Technology, Transactions of Civil Engineering*, vol. 44, pp. 179–191, 2020.

[14] N. D. Satyam and I. Towhata, "Site-specific ground response analysis and liquefaction assessment of Vijayawada city (India)," *Natural Hazards*, vol. 81, no. 2, pp. 705–724, 2016.

[15] M. Aaqib, S. Sadiq, D. Park, Y. M. Hashash, and M. Pehlivan, "Importance of implied strength correction for 1D site response at shallow sites at a moderate to low seismicity region," in *Proceedings of the Geotechnical Earthquake Engineering and Soil Dynamics V*, vol. 2018, pp. 445–453, ASCE, Austin, TX, USA, June 2018.

[16] M. Aaqib, D. Park, M. B. Adeel, Y. M. Hashash, and O. Ilhan, "Simulation-based site amplification model for shallow bedrock sites in Korea," *Earthquake Spectra*, vol. 37, no. 3, pp. 1900–1930, 2021.

[17] B. T. Nhung, N. H. Phuong, and N. T. Nam, "Assessment of earthquake-induced liquefaction hazard in urban areas of Hanoi city using LPI-based method," *Vietnam Journal of Earth Sciences*, vol. 40, no. 1, pp. 78–96, 2018.

[18] K.-L. Wen, C.-M. Lin, C.-H. Kuo, N. H. Phuong, N. T. Hung, and L. T. Son, "Site response analysis from microtremor survey in the Hanoi, Vietnam," in *Proceedings of the Geophysics-Cooperation and Sustainable Development*, Hanoi, Vietnam, November 2012.

[19] TCVN 9386: 2012, *Design of Structures for Earthquake Resistances*, CEN, Brussels, Belgium, in Vietnamese, 2012.

[20] R. Tuladhar, N. N. H. Cuong, and F. Yamazaki, "Seismic microzonation of Hanoi, Vietnam using microtremor observations," in *Proceedings of the 13th World Conference on Earthquake Engineering*, pp. 1–8, International Association of Earthquake Engineering, Vancouver, Canada, August 2004.

[21] S. Grasso and M. Maugeri, "The seismic microzonation of the city of Catania (Italy) for the maximum expected scenario

earthquake of January 11, 1693," *Soil Dynamics and Earthquake Engineering*, vol. 29, no. 6, pp. 953–962, 2009.

[22] Y. Hashash, M. I. Musgrove, J. A. Harmon et al., *Deepsoil 7.0, User Manual*, University of Illinois at Urbana-Champaign, Springfield, IL, USA, 2017.

[23] D.-D. Nguyen, D. Park, S. Shamsher, V.-Q. Nguyen, and T.-H. Lee, "Seismic vulnerability assessment of rectangular cut-and-cover subway tunnels," *Tunnelling and Underground Space Technology*, vol. 86, pp. 247–261, 2019.

[24] S. Sadiq, V. Q. Nguyen, H. Jung, and D. Park, "Effect of flexibility ratio on seismic response of cut-and-cover box tunnel," *Advances in Civil Engineering*, vol. 2019, Article ID 4905329, 16 pages, 2019.

[25] M. A. Sayed, O.-S. Kwon, D. Park, and Q. Van Nguyen, "Multi-platform soil-structure interaction simulation of Daikai subway tunnel during the 1995 Kobe earthquake," *Soil Dynamics and Earthquake Engineering*, vol. 125, Article ID 105643, 2019.

[26] V.-Q. Nguyen, Z. A. Nizamani, D. Park, and O.-S. Kwon, "Numerical simulation of damage evolution of Daikai station during the 1995 Kobe earthquake," *Engineering Structures*, vol. 206, Article ID 110180, 2020.

[27] D. R. Groholski, Y. M. Hashash, B. Kim, M. Musgrove, J. Harmon, and J. P. Stewart, "Simplified model for small-strain nonlinearity and strength in 1D seismic site response analysis," *Journal of Geotechnical and Geoenvironmental Engineering*, vol. 142, no. 9, Article ID 04016042, 2016.

[28] Y. M. Hashash, S. Dashti, M. Musgrove et al., "Influence of tall buildings on seismic response of shallow underground structures," *Journal of Geotechnical and Geoenvironmental Engineering*, vol. 144, no. 12, Article ID 04018097, 2018.

[29] N. Ntritsos and M. Cubrinovski, "A CPT-based effective stress analysis procedure for liquefaction assessment," *Soil Dynamics and Earthquake Engineering*, vol. 131, Article ID 106063, 2020.

[30] J. D. Bray and J. Macedo, "6th Ishihara lecture: simplified procedure for estimating liquefaction-induced building settlement," *Soil Dynamics and Earthquake Engineering*, vol. 102, pp. 215–231, 2017.

[31] M. B. Darendeli, *Development of a new family of normalized modulus reduction and material damping curves*, Ph.D. dissertation, University of Texas at Austin, Austin, TX, USA, 2001.

[32] J. Rey, E. Faccioli, and J. J. Bommer, "Derivation of design soil coefficients (S) and response spectral shapes for Eurocode 8 using the European strong-motion database," *Journal of Seismology*, vol. 6, no. 4, pp. 547–555, 2002.

[33] K. Pitilakis, E. Riga, A. Anastasiadis, S. Fotopoulou, and S. Karafagka, "Towards the revision of EC8: proposal for an alternative site classification scheme and associated intensity dependent spectral amplification factors," *Soil Dynamics and Earthquake Engineering*, vol. 126, Article ID 105137, 2019.

[34] FEMA P-1050-1, "NEHRP recommended seismic provisions for new buildings and other structures, volume 1: part 1 provisions, part 2 commentary," 2015, https://www.fema.gov/sites/default/files/2020-07/fema_nehrp-seismic-provisions-new-buildings_p-1050-1_2015.pdf.

[35] J. Kaklamanos, L. G. Baise, E. M. Thompson, and L. Dorfmann, "Comparison of 1D linear, equivalent-linear, and nonlinear site response models at six KiK-net validation sites," *Soil Dynamics and Earthquake Engineering*, vol. 69, pp. 207–219, 2015.